Handbook of Electrochemical Impedance Spectroscopy Transfert functions

Technical Report · January 2020

DOI: 10.13140/RG.2.2.24475.62240

3 authors, including:

Jean-Paul Diard
BioLogic
219 PUBLICATIONS **2,580** CITATIONS

Bernard Le Gorrec
UJFG-INPG
108 PUBLICATIONS **1,450** CITATIONS

Handbook
of
Electrochemical Impedance Spectroscopy

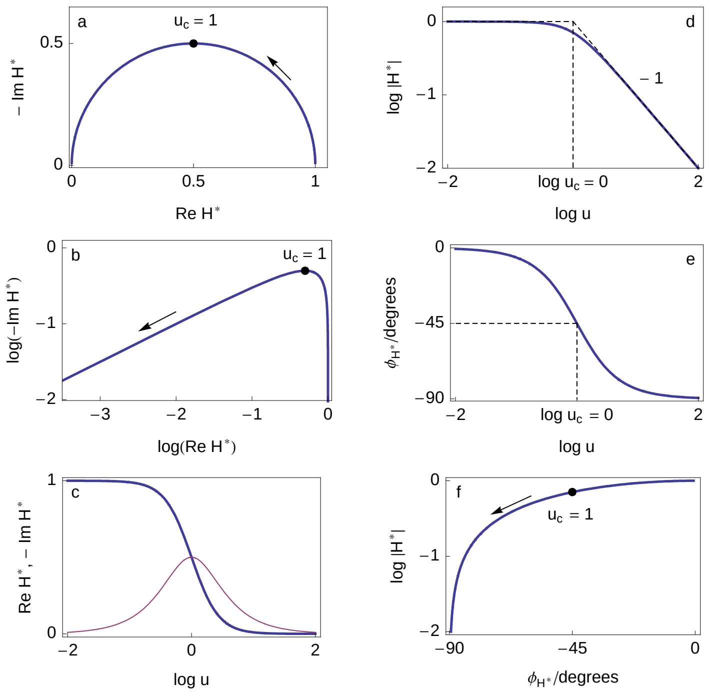

TRANSFER FUNCTIONS

ER@SE/LEPMI
J.-P. Diard, B. Le Gorrec, C. Montella

Hosted by Bio-Logic @ `www.bio-logic.info`

December 21, 2013

Contents

Chapter 1

Graphs of transfer functions

1.1 Introduction [1]

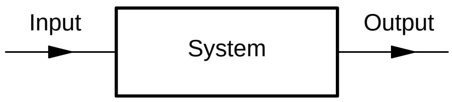

Figure 1.1: Sketch of a scalar system.

- The transfer function, H, of a invariant scalar linear system is given by:

  $$H(s) = \frac{\mathcal{L}[\text{Output}]}{\mathcal{L}[\text{Input}]}$$

  $\mathcal{L}$ denotes the Laplace transform, s is the Laplace variable with $s = \sigma + \mathrm{i}\,\omega$. For current input and potential output, H is an impedance.

- A transfer function is a complex fonction $H(s)$ of two real variables σ and ω. It is not possible to plot graph of $H(s)$ in a plane, only 3D-plots are possible [4] (cf. Chap. 4).

- For $s = \mathrm{i}\,\omega$, *i.e.* $\sigma = 0$, corresponding to frequencial analysis, a transfer function is a complex fonction $H = H(\mathrm{i}\,\omega)$ (or $H(\omega)$) of a real variable ω. It is possible to plot graph of $H = H(\omega)$ in a plane and different types of graph can be used.

- The order of rational fraction transfer function is the degree in s (or $\mathrm{i}\,\omega$) of the transfer function denominator.
  - The relativer order of rational fraction transfer function is the difference between the order of the denominator and the order of the numerator.
  - A proper system is a system where the degree of the denominator is larger or equal to the degree of the numerator.
  - A strictly proper system is a system where the degree of the denominator is larger than the degree of the numerator.

- Poles of transfer function are the roots of the denominator of the transfer function $H(s)$.
  - Dominant poles: poles closest to the imaginary axis
- Zeros of transfer function are the roots of the numerator of the transfer function $H(s)$.

1.2 Nyquist diagram

1.2.1 Nyquist diagram used by electricians

Orthonormal parametric plot

$$x = \mathrm{Re}\ H = f(\omega),\ y = \mathrm{Im}\ H = g(\omega) \tag{1.1}$$

1.2.2 Nyquist diagram used by electrochemists

Orthonormal parametric plot

$$x = \mathrm{Re}\ H = f(\omega),\ y = -\mathrm{Im}\ H = g(\omega) \tag{1.2}$$

1.3 Bode diagram

1.3.1 Bode diagram used by electricians

- Modulus diagram: $20\ \log|H|\ vs.\ \log\omega$. $|H|$ is the modulus (or magnitude or amplitude) of H with $|H| = \sqrt{(\mathrm{Re}\ H)^2 + (\mathrm{Im}\ H)^2}$.
- Phase diagram: $\phi_{\mathrm{H}}\ vs.\ \log\omega$. ϕ_{H} is the phase of H with $\phi_{\mathrm{H}} = \arctan\dfrac{\mathrm{Im}\ H}{\mathrm{Re}\ H}$

1.3.2 Bode diagram used by electrochemists

$$\log|H|\ vs.\ \log\omega,\ \phi_{\mathrm{H}}\ vs.\ \log\omega \tag{1.3}$$

1.4 Black diagram

1.4.1 Black diagram used by electrician

Parametric plot

$$x = \phi_{\mathrm{H}} = f(\omega),\ y = 20\ \log|H| = g(\omega) \tag{1.4}$$

1.4.2 Black diagram used by electrochemists

Parametric plot

$$x = \phi_{\mathrm{H}} = f(\omega),\ y = \log|H| = g(\omega) \tag{1.5}$$

1.5 Miscellaneous

- $\mathrm{Re}\, H$ *vs.* $\log \omega$, $\mathrm{Im}\, H$ *vs.* $\log \omega$,
- $\log \mathrm{Re}\, H$ *vs.* $\log \omega$, $\log \mathrm{Im}\, H$ *vs.* $\log \omega$ [12, 11],
- $\log \mathrm{Im}\, H$ *vs.* $\log \mathrm{Re}\, H$ [7, 2], $\log |\mathrm{Im}\, H|$ *vs.* $\log |\mathrm{Re}\, H|$,
- $\log \mathrm{Im}\, H$ *vs.* $\mathrm{Re}\, H$ [9, 2].

Chapter 2

First-order and generalized first-order transfer functions

2.1 First-order transfer function [3, 8]

2.1.1 First-order transfer function

$$H(s) = \frac{K}{1 + \tau s},\ H(\omega) = \frac{K}{1 + \mathrm{i}\,\omega\,\tau}$$

K: static gain, τ: time constant.

2.1.2 Dimensionless first-order transfer function

$$H^*(S) = \frac{H(s)}{K} = \frac{1}{1 + S},\ S = \tau\, s = \Sigma + \mathrm{i}\, u,\ \Sigma = \tau\, \sigma,\ u = \tau\, \omega$$

One real pole: $S_{\mathrm{p}} = -1$ (Fig. 2.1).

$$H^*(u) = \frac{H(\omega)}{K} = \frac{1}{1 + \mathrm{i}\, u},\ u = \tau\, \omega \tag{2.1}$$

u: reduced (or dimensionless or nondimensional) angular (or radial) frequency

$$\mathrm{Re}\, H^*(u) = \frac{1}{1 + u^2},\ \mathrm{Im}\, H^*(u) = -\frac{u}{1 + u^2},\ \lim_{u \to 0} \mathrm{Re}\, H^*(u) = 1$$

Characteristic frequency: $u_{\mathrm{c}} = 1$ (Fig. 2.1).

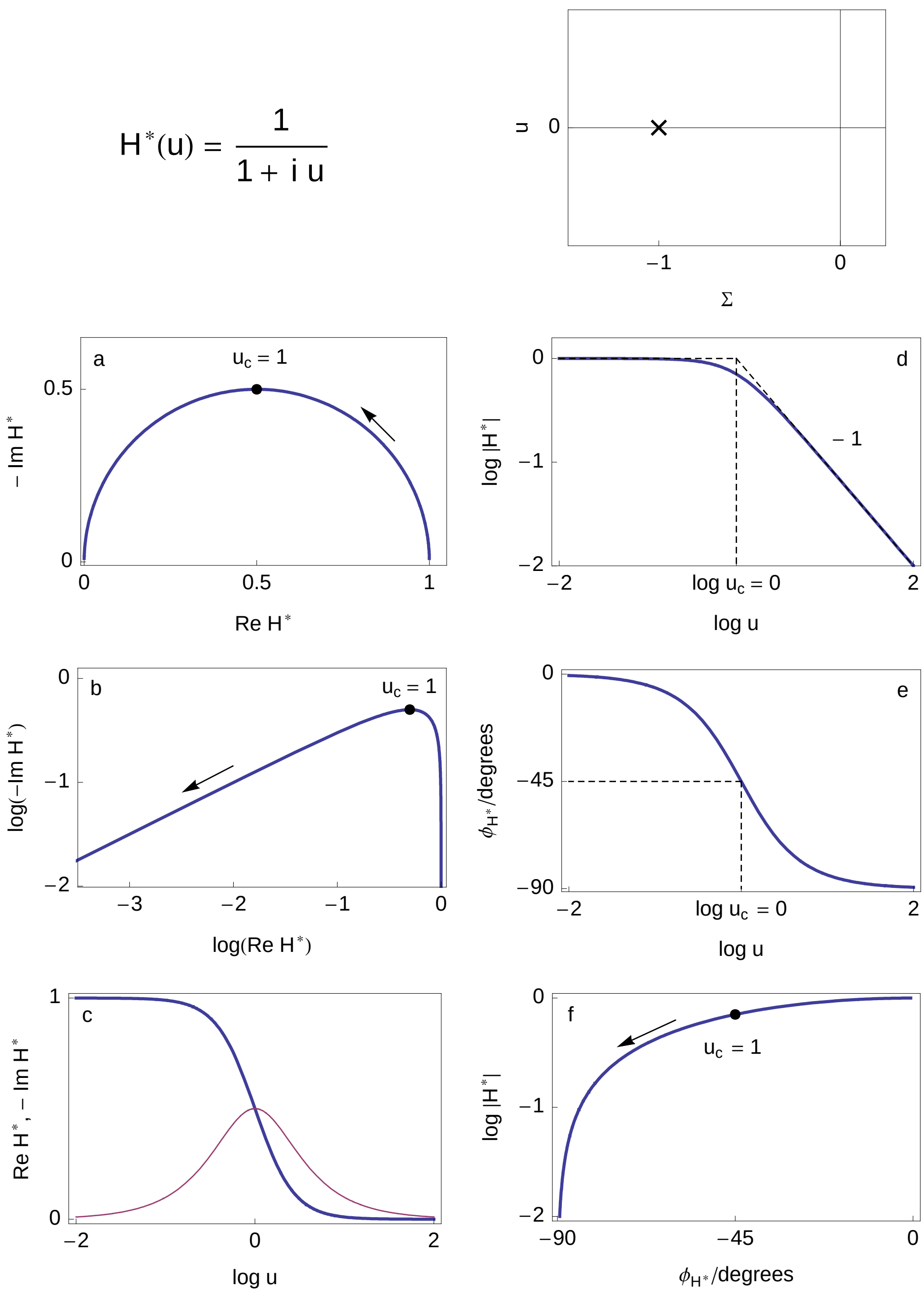

Figure 2.1: Pole-zero map, Nyquist (a), log Nyquist (b) Re H^* *vs.* $\log u$ (c, thick line), $-\mathrm{Im}\, H^*$ *vs.* $\log u$ (c, thin line), Bode (modulus (c) and phase (d)) and Black diagrams of the first order transfer function $H^*(u) = 1/(1+\mathrm{i}\,u)$. Arrow always indicates increasing angular frequencies.

2.2 Generalized first-order transfer functions

2.2.1 High-pass first-order transfer function

$$H(s) = \frac{K\,\tau_{\mathrm{N}}\,s}{1+\tau_{\mathrm{D}}\,s},\ H(\omega) = \frac{K\,\tau_{\mathrm{N}}\,\mathrm{i}\,\omega}{1+\tau_{\mathrm{D}}\,\mathrm{i}\,\omega}$$

2.2.2 Dimensionless high-pass first-order transfer function

$$H^*(S) = \frac{H(s)}{K\,r_\tau} = \frac{S}{1+S},\ r_\tau = \frac{\tau_{\mathrm{N}}}{\tau_{\mathrm{D}}},\ S = \tau_{\mathrm{D}}\,s = \Sigma + \mathrm{i}\,u,\ \Sigma = \tau_{\mathrm{D}}\,\sigma,\ u = \tau_{\mathrm{D}}\,w$$

One real pole: $S_{\mathrm{p}} = -1$, one zero at the origin: $S_{\mathrm{z}} = 0$ (Fig. 2.2).

$$H^*(u) = \frac{H(\omega)}{r_\tau} = \frac{\mathrm{i}\,u}{1+\mathrm{i}\,u},\ u = \tau_{\mathrm{D}}\,\omega$$

$$\mathrm{Re}\ H^*(u) = \frac{u^2}{1+u^2},\ \mathrm{Im}\ H^*(u) = \frac{u}{1+u^2}$$

$$\lim_{u\to\infty} \mathrm{Re}\ H^*(u) = 1$$

Characteristic frequency: $u_{\mathrm{c}} = 1$ (Fig. 2.2).

2.2.3 Generalized first-order transfer function

$$H(s) = \frac{K\,(1+\tau_{\mathrm{N}}\,s)}{1+\tau_{\mathrm{D}}\,s},\ H(\omega) = \frac{K\,(1+\tau_{\mathrm{N}}\,\mathrm{i}\,\omega)}{1+\tau_{\mathrm{D}}\,\mathrm{i}\,\omega}$$

2.2.4 Dimensionless generalized first-order transfer function

$$H^*(S) = \frac{H(S)}{K} = \frac{1+r_\tau\,S}{1+S},\ r_\tau = \frac{\tau_{\mathrm{N}}}{\tau_{\mathrm{D}}},\ S = \tau_{\mathrm{D}}\,s = \Sigma + \mathrm{i}\,u,\ \Sigma = \tau_{\mathrm{D}}\,\sigma,\ u = \tau_{\mathrm{D}}\,\omega$$

One real pole: $S_{\mathrm{p}} = -1 = -u_{\mathrm{c1}}$, one real zero: $S_{\mathrm{z}} = -1/r_\tau = -u_{\mathrm{c2}}$.

$$H^*(u) = \frac{H(u)}{K} = \frac{1+\mathrm{i}\,r_\tau\,u}{1+\mathrm{i}\,u}$$

$$\mathrm{Re}\ H^*(u) = \frac{1+r_\tau\,u^2}{1+u^2},\ \mathrm{Im}\ H^*(u) = \frac{(-1+r_\tau)\ u}{1+u^2}$$

$$\lim_{u\to 0} \mathrm{Re}\ H^*(u) = 1,\ \lim_{u\to\infty} \mathrm{Re}\ H^*(u) = r_\tau$$

Characteristic frequency: $u_{\mathrm{c1}} = 1,\ u_{\mathrm{c2}} = 1/r_\tau$ ($\phi_{u_{\mathrm{c1}}} = \phi_{u_{\mathrm{c2}}}$).

$r_\tau < 1 \Rightarrow$ Capacitive behaviour (Fig. 2.3).
$r_\tau > 1 \Rightarrow$ Inductive behaviour (Fig. 2.4).

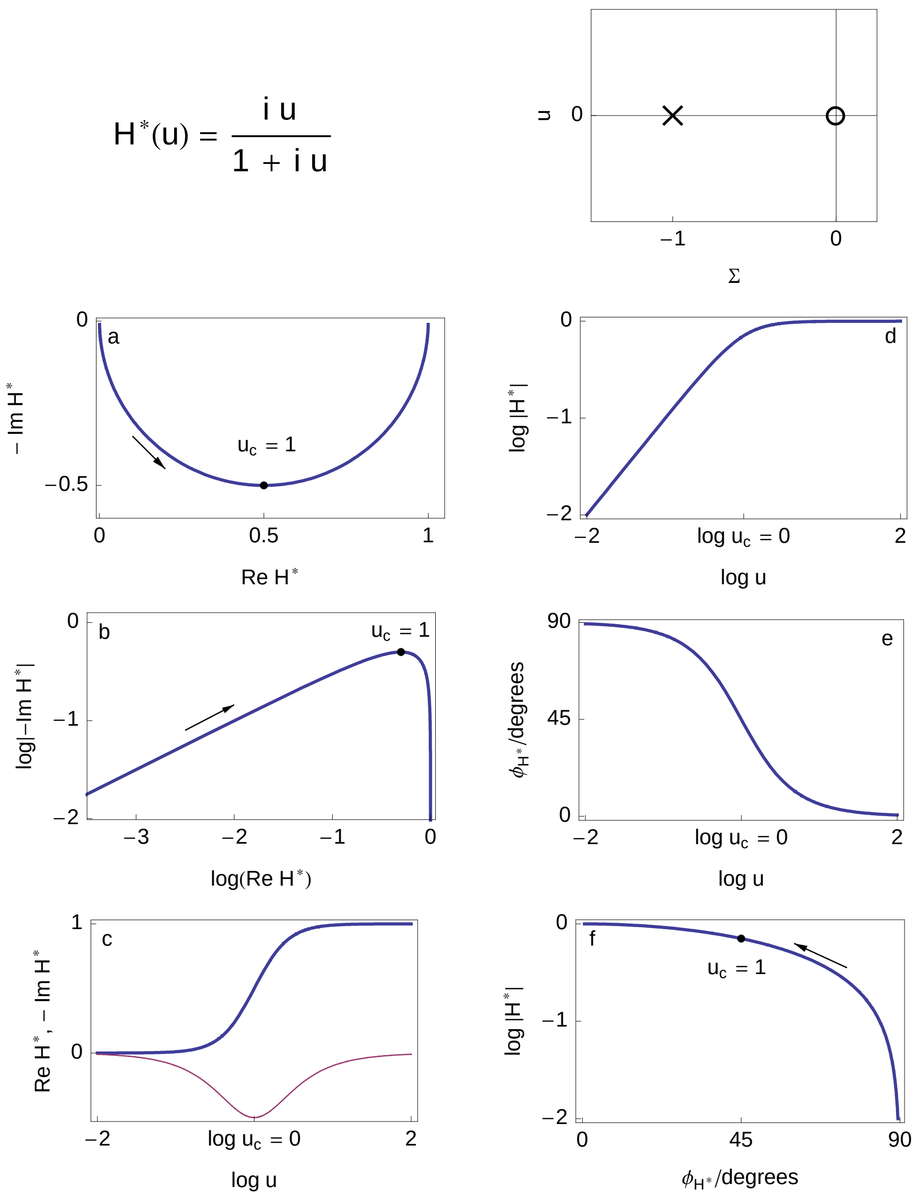

Figure 2.2: Pole-zero map, Nyquist (a), log Nyquist (b) Re H^* *vs.* $\log u$ (c, thick line), $-$Im H^* *vs.* $\log u$ (c, thin line), Bode (modulus (c) and phase (d)) and Black diagrams of the high-pass first-order transfer function. Arrow always indicates increasing angular frequencies.

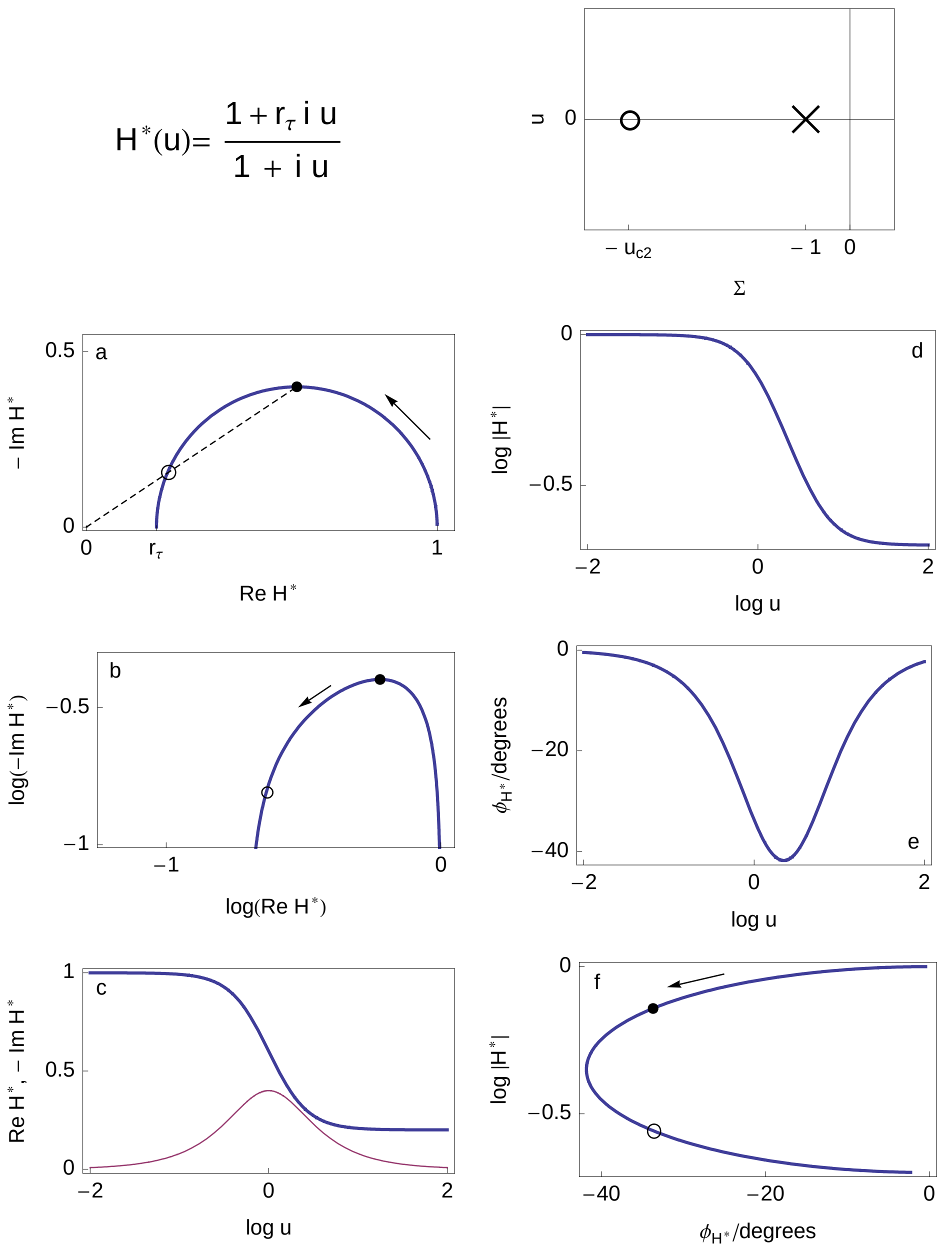

Figure 2.3: Pole-zero map, Nyquist (a), log Nyquist (b) Re H^* *vs.* $\log u$ (c, thick line), $-\text{Im}\ H^*$ *vs.* $\log u$ (c, thin line), Bode (modulus (c) and phase (d)) and Black diagrams of the generalized first order transfer function. $r_\tau = 0.2$ ($r_\tau < 1$), dot: $u_{c1} = 1$, circle: $u_{c2} = 1/r_\tau$.

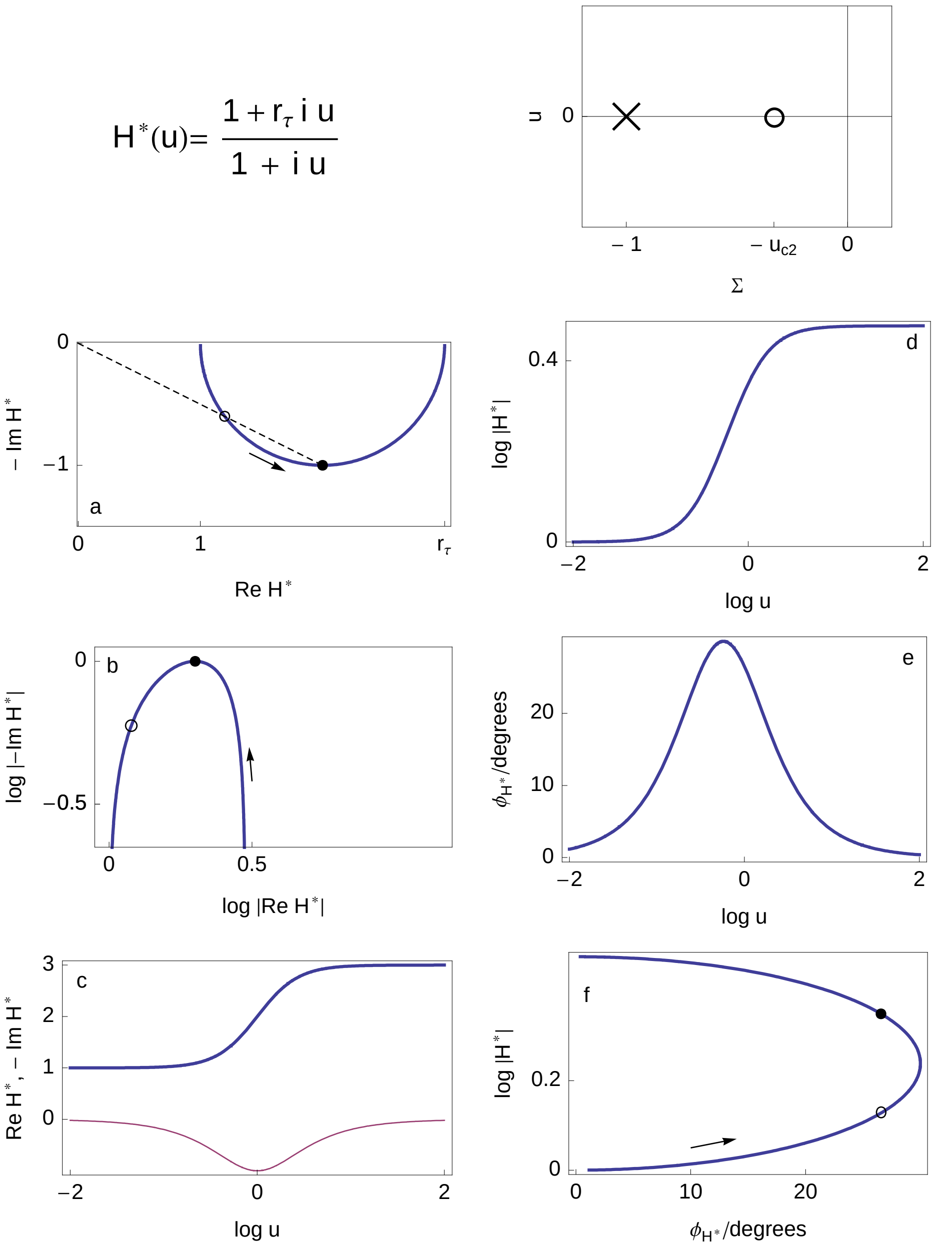

Figure 2.4: Pole-zero map, Nyquist (a), log Nyquist (b) Re H^* *vs.* $\log u$ (c, thick line), $-\mathrm{Im}\ H^*$ *vs.* $\log u$ (c, thin line), Bode (modulus (c) and phase (d)) and Black diagrams of the generalized first order transfer function. $r_\tau = 3$ ($r_\tau > 1$), dot: $u_{c1} = 1$, circle: $u_{c2} = 1/r_\tau$.

Chapter 3

Second-order and generalized second-order transfer functions

3.1 Introduction

$$H(s) = \frac{K}{1 + a_1\, s + a_2\, s^2}$$

3.1.1 Canonical form

$$H(s) = \frac{K}{1 + 2\,\zeta\,\dfrac{s}{\omega_\mathrm{n}} + \left(\dfrac{s}{\omega_\mathrm{n}}\right)^2}$$

poles:

$$s_{\mathrm{p1}} = -\zeta\omega_\mathrm{n} - \sqrt{(\zeta^2 - 1)\,\omega_\mathrm{n}^2},\ s_{\mathrm{p2}} = -\zeta\omega_\mathrm{n} + \sqrt{(\zeta^2 - 1)\,\omega_\mathrm{n}^2}$$

- $\zeta > 1$, two real poles
- $\zeta = 1$ multiple pole
- $\zeta < 1$ complex poles

3.1.2 Reduced form

$$H^*(S) = \frac{H(s)}{K} = \frac{1}{1 + 2\,\zeta\, S + S^2},\ S = \frac{s}{\omega_\mathrm{n}} = \frac{\sigma + \mathrm{i}\,\omega}{\omega_\mathrm{n}} = \Sigma + \mathrm{i}\, u,\ \Sigma = \frac{\sigma}{\omega_\mathrm{n}},\ u = \frac{\omega}{\omega_\mathrm{n}}$$

poles:

$$S_{\mathrm{p1}} = -\zeta - \sqrt{\zeta^2 - 1},\ S_{\mathrm{p2}} = -\zeta + \sqrt{\zeta^2 - 1}$$

3.1.3 Second-order transfer function with real poles

$$H(s) = \frac{K}{(1+\tau_1\,s)\,(1+\tau_2\,s)},\ H(\omega) = \frac{K}{(1+\tau_1\,\mathrm{i}\,\omega)\,(1+\tau_2\,\mathrm{i}\,\omega)}$$

$$H^*(S) = \frac{H(s)}{K} = \frac{1}{(1+S)\,(1+r_\tau\,S)},\ S = \tau_1\,s = \Sigma + \mathrm{i}\,u,\ \Sigma = \tau_1\,\sigma,\ u = \tau_1\,\omega,\ \ r_\tau = \frac{\tau_2}{\tau_1}$$

Two real poles: $S_{\mathrm{p1}} = -1 = -u_{\mathrm{c1}}$, $S_{\mathrm{p2}} = -1/r_\tau = -u_{\mathrm{c2}}$ (Fig. 3.1).

$$H^*(u) = \frac{1}{(1+\mathrm{i}\,u)\,(1+r_\tau\,\mathrm{i}\,u)}$$

$$\mathrm{Re}\,H^*(u) = \frac{1-u^2\,r_\tau}{(1+u^2)\,\left(1+u^2\,{r_\tau}^2\right)},\ \mathrm{Im}\,H^*(u) = -\frac{u\,(1+r_\tau)}{(1+u^2)\,\left(1+u^2\,{r_\tau}^2\right)}$$

3.1.4 Second-order transfer function with complex poles

$$H^*(S) = \frac{1}{1+2\,\zeta\,S+S^2},\ \zeta < 1$$

Two complex poles (Fig. 3.2) :

$$S_{\mathrm{p1}} = -\zeta - \sqrt{\zeta^2-1} = -\zeta - \mathrm{i}\,\sqrt{1-\zeta^2},\ S_{\mathrm{p2}} = -\zeta + \sqrt{\zeta^2-1} = -\zeta + \mathrm{i}\,\sqrt{1-\zeta^2}$$

$$H^*(u) = \frac{1}{1+2\,\zeta\,\mathrm{i}\,u+(\mathrm{i}\,u)^2},\ \zeta < 1$$

$$\mathrm{Re}\,H^*(u) = \frac{1-u^2}{u^4+(4\zeta^2-2)\,u^2+1},\ \mathrm{Im}\,H^*(u) = -\frac{2u\zeta}{u^4+(4\zeta^2-2)\,u^2+1}$$

3.1.5 Second-order transfer function with multiple poles

$$H^*(S) = \frac{1}{1+2\,\zeta\,S+S^2},\ \zeta = 1 \Rightarrow H^*(S) = \frac{1}{(1+S)^2}$$

One multiple pole: $S_{\mathrm{p}} = -1 \Rightarrow u_{\mathrm{c}} = 1$ (Fig. 3.3).

$$H^*(u) = \frac{1}{(1+\mathrm{i}\,u)^2}$$

$$\mathrm{Re}\,H^*(u) = \frac{1-u^2}{\left(u^2+1\right)^2},\ \mathrm{Im}\,H^*(u) = -\frac{2u}{\left(u^2+1\right)^2}$$

$$\frac{\mathrm{dIm}\,(u)}{\mathrm{d}u} = 0 \Rightarrow \omega = \frac{1}{\sqrt{3}},\ H^*(u) = \frac{3}{8}\,(1-\mathrm{i}\,\sqrt{3})$$

$$\frac{\mathrm{dRe}\,(u)}{\mathrm{d}u} = 0 \Rightarrow \omega = \sqrt{3},\ H^*(u) = -\frac{1}{8}\,(1+\mathrm{i}\,\sqrt{3})$$

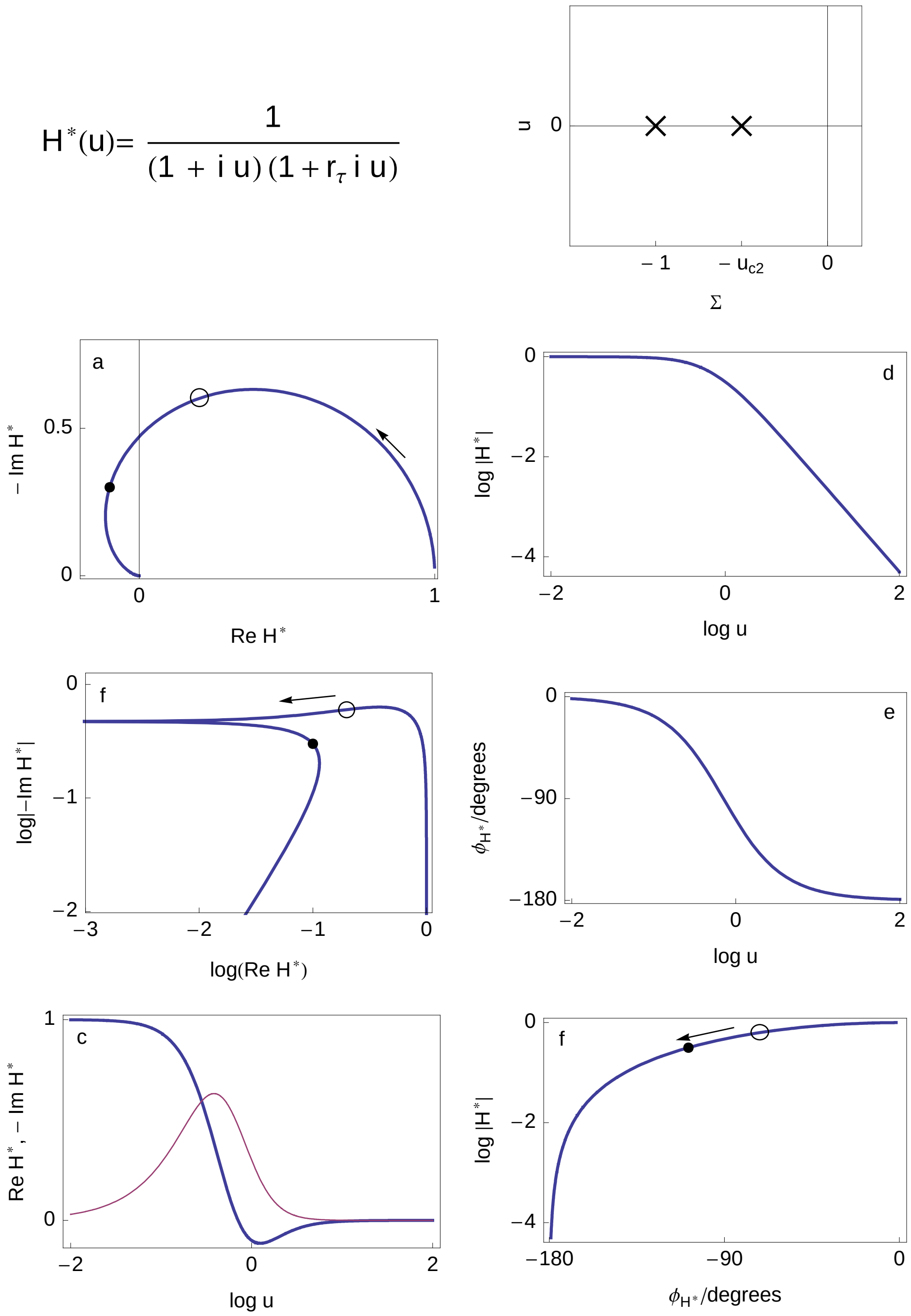

Figure 3.1: Pole-zero map, Nyquist (a), log Nyquist (b) Re H^* *vs.* $\log u$ (c, thick line), $-\mathrm{Im}\ H^*$ *vs.* $\log u$ (c, thin line), Bode (modulus (c) and phase (d)) and Black diagrams of the reduced second order transfer function with real poles $H^* = 1/((1 + \mathrm{i}\,u)\,(1 + r_\tau\,\mathrm{i}\,u))$. $r_\tau = 2$ ($r_\tau > 1$), dot: $u_{c1} = 1$, circle: $u_{c2} = 1/r_\tau$.

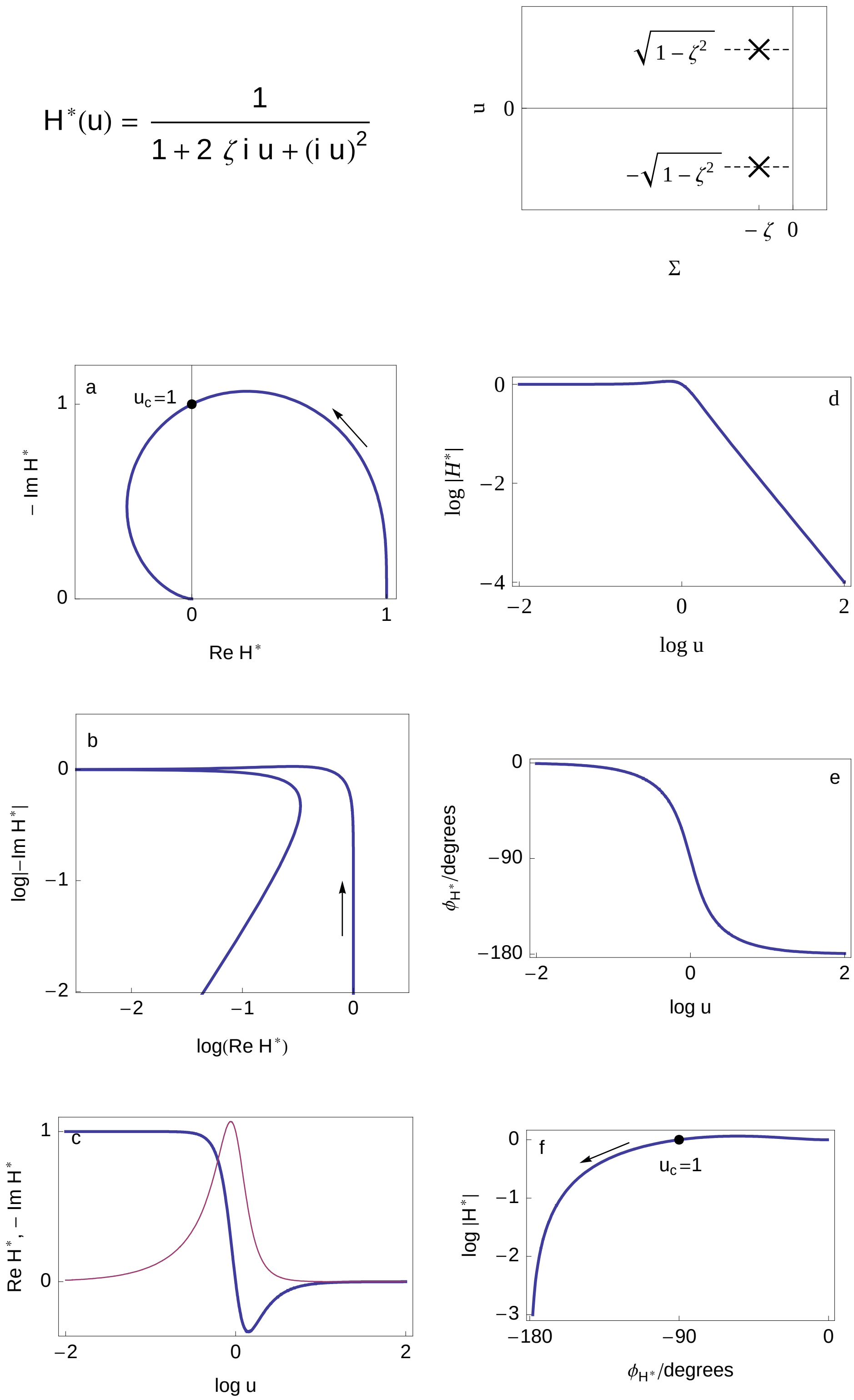

Figure 3.2: Pole-zero map, Nyquist (a), log Nyquist (b) Re H^* *vs.* $\log u$ (c, thick line), $-$Im H^* *vs.* $\log u$ (c, thin line), Bode (modulus (c) and phase (d)) and Black diagrams of the reduced second order transfer function with complex poles $H^*(u) = 1/(1 + 2\,\zeta\,\mathrm{i}\,u + (\mathrm{i}\,u)^2)$, $\zeta = 0.5$.

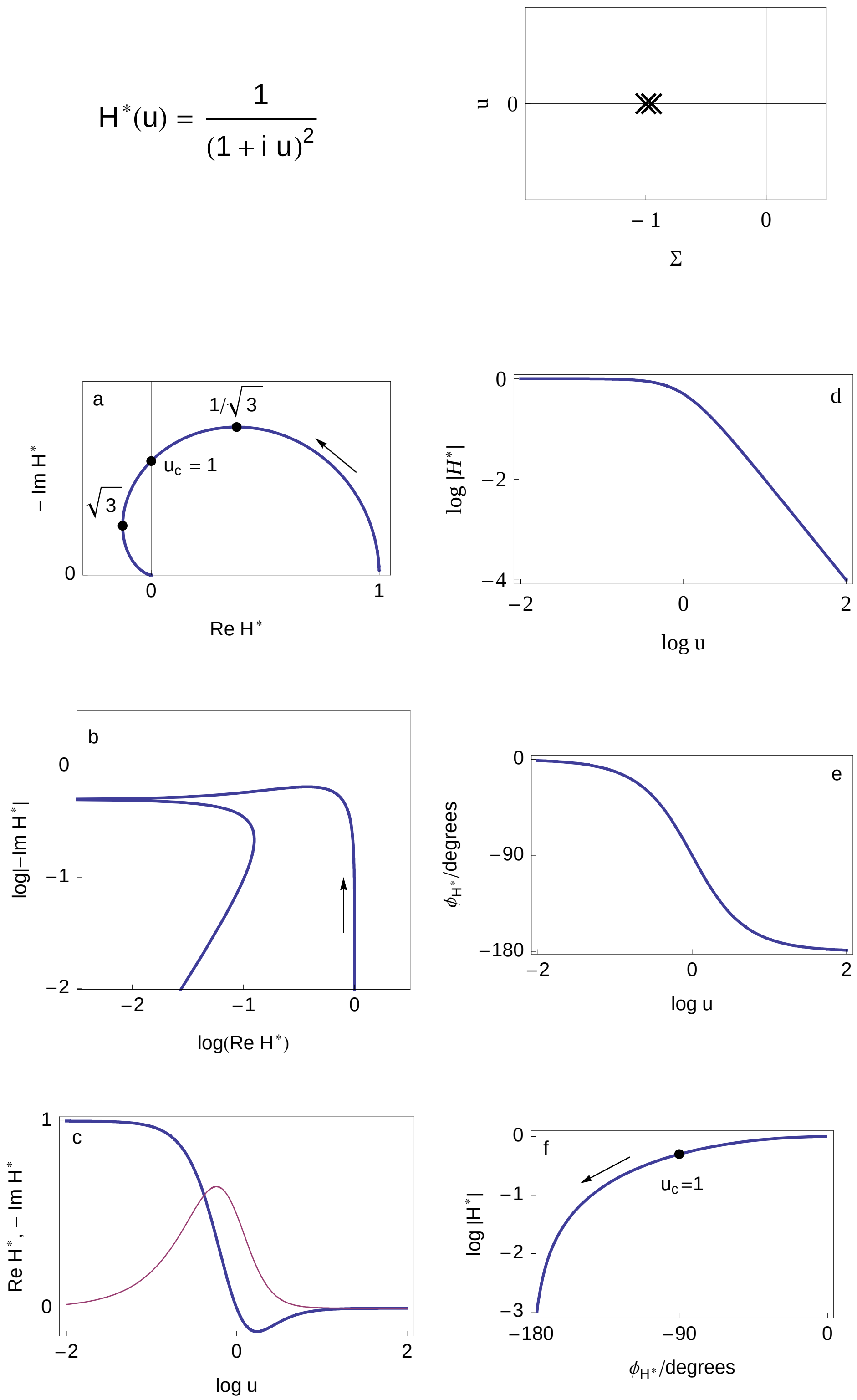

Figure 3.3: Pole-zero map, Nyquist (a), log Nyquist (b) Re H^* *vs.* $\log u$ (c, thick line), $-\mathrm{Im}\,H^*$ *vs.* $\log u$ (c, thin line), Bode (modulus (c) and phase (d)) and Black diagrams of the reduced second order transfer function with multiple poles $H^*(u) = 1/(1 + \mathrm{i}\,u)^2$.

3.2 Generalized second-order transfer functions

3.2.1 Generalized second-order transfer functions

$$H(s) = \frac{K\,(1 + b_1\,s)}{1 + a_1\,s + a_2\,s^2}$$

3.2.2 Electrochemical examples

Volmer-Heyrovský reaction with chemical desorption [10, 5, 6]

$$\mathrm{A^+ + s + e^-} \xrightarrow{K_{\mathrm{r1}}} \mathrm{A,s}$$

$$\mathrm{A^+ + A,s + e^-} \xrightarrow{K_{\mathrm{r2}}} \mathrm{A_2,s}$$

$$\mathrm{A_2,s} \xrightarrow{k_{\mathrm{d3}}} \mathrm{A_2 + s}$$

Schuhmann dissolution-passivation reaction # 1 [13]

$$\mathrm{M,s} \underset{K_{\mathrm{r1}}}{\overset{K_{\mathrm{o1}}}{\longleftrightarrow}} \mathrm{X,s + 2\ e}$$

$$\mathrm{X,s} \underset{K_{\mathrm{r2}}}{\overset{K_{\mathrm{o2}}}{\longleftrightarrow}} \mathrm{Q,s + 2\ e}$$

$$\mathrm{X,s + A} \xrightarrow{K_{\mathrm{o3}}} \mathrm{X,s + B + 2\ e}$$

3.2.3 Canonical form

$$H(s) = \frac{K\,(1 + b_1\,s)}{1 + 2\,\zeta\,\dfrac{s}{\omega_\mathrm{n}} + \left(\dfrac{s}{\omega_\mathrm{n}}\right)^2}$$

poles:

$$s_{\mathrm{p1}} = -\zeta\omega_\mathrm{n} - \sqrt{(\zeta^2 - 1)\,\omega_\mathrm{n}^2},\ s_{\mathrm{p2}} = -\zeta\omega_\mathrm{n} + \sqrt{(\zeta^2 - 1)\,\omega_\mathrm{n}^2}$$

$\zeta > 1$, two real poles, $\zeta = 1$ multiple pole, $\zeta < 1$ complex poles (cf. 3.1.1).

3.2.4 Reduced form

$H^*(S) = \dfrac{H(s)}{K} = \dfrac{1 + T\,S}{1 + 2\,\zeta\,S + S^2},\ S = \dfrac{s}{\omega_\mathrm{n}} = \dfrac{\sigma + \mathrm{i}\,\omega}{\omega_\mathrm{n}} = \Sigma + \mathrm{i}\,u,\ \Sigma = \dfrac{\sigma}{\omega_\mathrm{n}},\ u = \dfrac{\omega}{\omega_\mathrm{n}}$

poles: $S_{\mathrm{p1}} = -\zeta - \sqrt{\zeta^2 - 1}$, $S_{\mathrm{p2}} = -\zeta + \sqrt{\zeta^2 - 1}$, zero: $S_z = -1/T$.

$$\mathrm{Re}\,H^*(u) = \frac{(2T\zeta - 1)u^2 + 1}{u^4 + (4\zeta^2 - 2)\,u^2 + 1},\ \mathrm{Im}\,H^*(u) = \frac{u\left(-Tu^2 + T - 2\zeta\right)}{u^4 + (4\zeta^2 - 2)\,u^2 + 1}$$

$\Rightarrow$ Im $H^*(u) > 0$ (inductif behaviour) for $0 < u < \sqrt{T - 2\,\zeta}/\sqrt{T}$ if $T > 2\,\zeta$.

3.2.5 Complex poles $\zeta < 1$

- $T > 1$: Fig. 3.4,
- $T = 1$: Fig. 3.5,
- $T < 1$: Figs. 3.6 and 3.7.

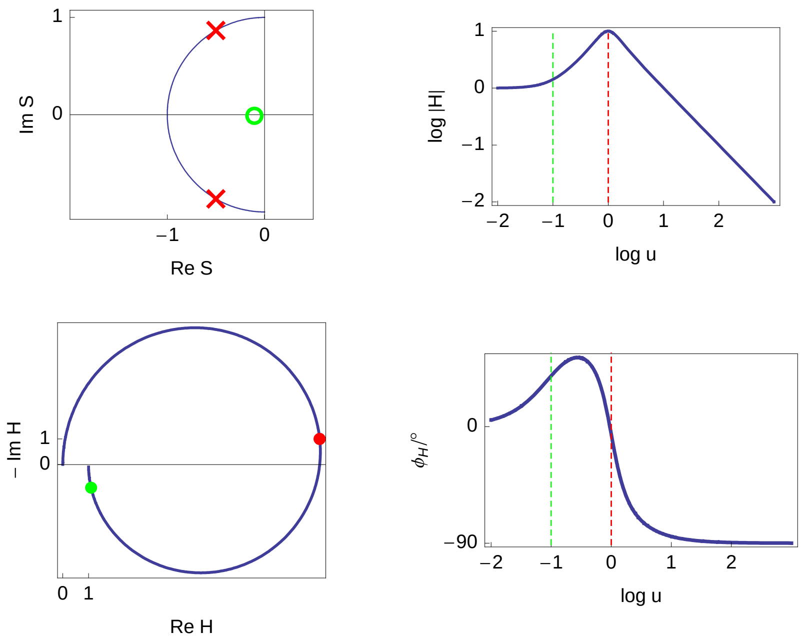

Figure 3.4: Pole-zero map, Nyquist, Bode (modulus and phase) of the reduced generalized second-order transfer function with complex poles $H^*(u) = (1+T\,\mathrm{i}\,u)/(1+2\,\zeta\,\mathrm{i}\,u+(\mathrm{i}\,u)^2)$. $\zeta = 0.5$, $T = 10$.

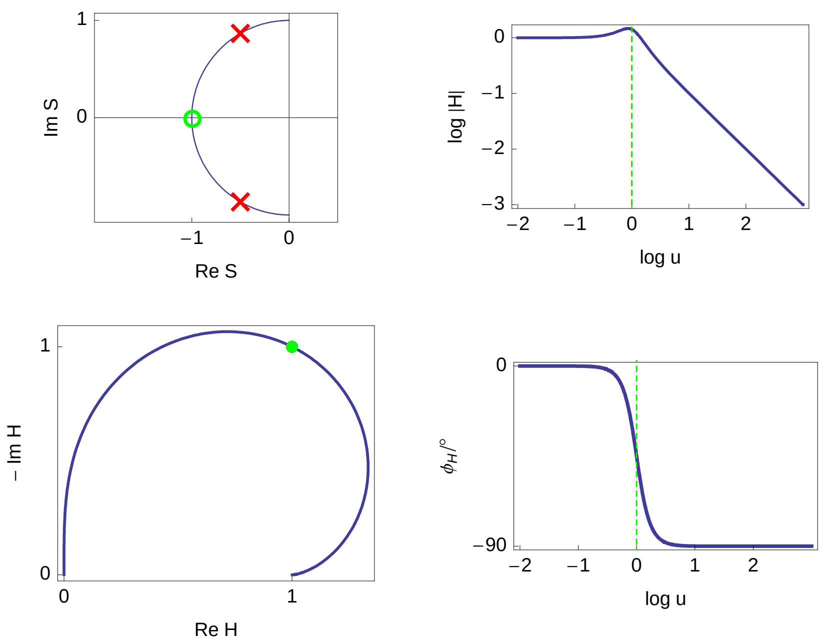

Figure 3.5: Pole-zero map, Nyquist, Bode (modulus and phase) of the reduced generalized second-order transfer function with complex poles $H^*(u) = (1+T\,\mathrm{i}\,u)/(1+2\,\zeta\,\mathrm{i}\,u+(\mathrm{i}\,u)^2)$. $\zeta = 0.5$, $T = 1$.

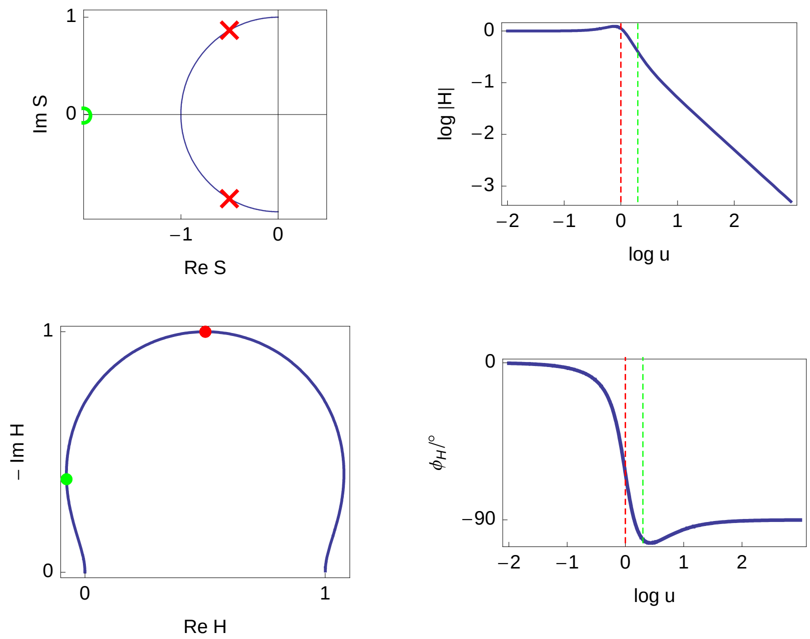

Figure 3.6: Pole-zero map, Nyquist, Bode (modulus and phase) of the reduced generalized second-order transfer function with complex poles $H^*(u) = (1 + T\,\mathrm{i}\,u)/(1 + 2\,\zeta\,\mathrm{i}\,u + (\mathrm{i}\,u)^2)$. $\zeta = 0.5$, $T = 0.5$.

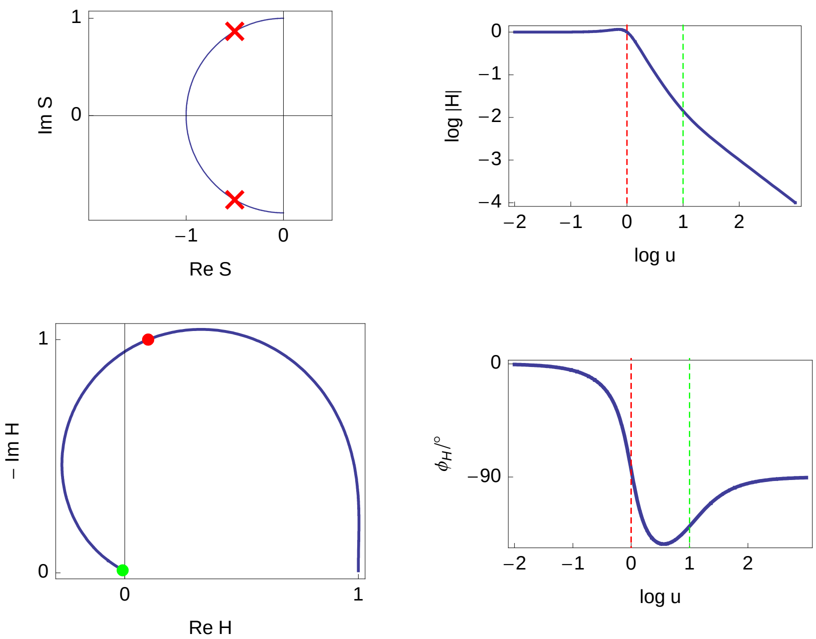

Figure 3.7: Pole-zero map, Nyquist, Bode (modulus and phase) of the reduced generalized second-order transfer function with complex poles $H^*(u) = (1 + T\,\mathrm{i}\,u)/(1 + 2\,\zeta\,\mathrm{i}\,u + (\mathrm{i}\,u)^2)$. $\zeta = 0.5$, $T = 0.1$. Zero not shown in the pole-zero map.

3.2.6 Multiple poles $\zeta = 1$

- $T > 1$: Fig. 3.8,
- $T = 1$: Fig. 3.9,
- $T < 1$: Fig. 3.10.

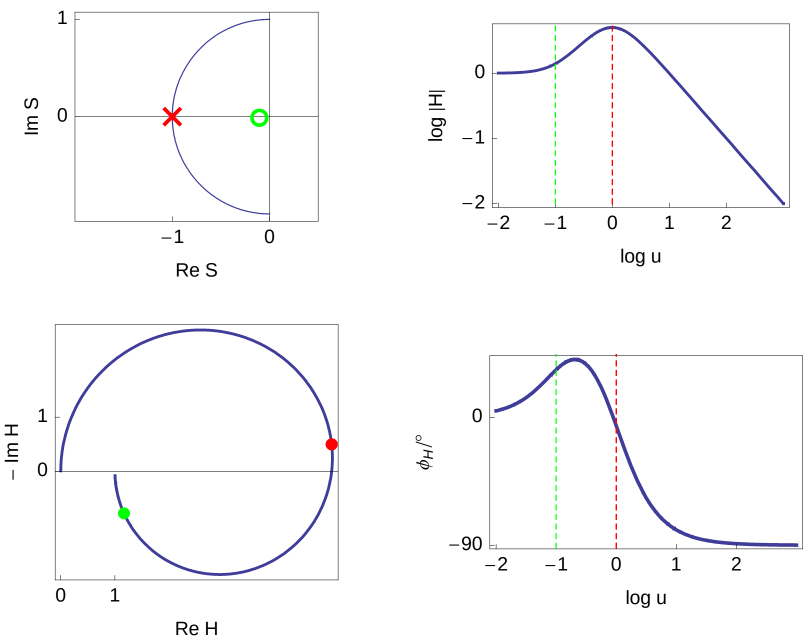

Figure 3.8: Pole-zero map, Nyquist, Bode (modulus and phase) of the reduced generalized second-order transfer function with multiple poles $H^*(u) = (1 + T\,\mathrm{i}\,u)/(1 + 2\,\zeta\,\mathrm{i}\,u + (\mathrm{i}\,u)^2)$. $\zeta = 1$, $T = 10$.

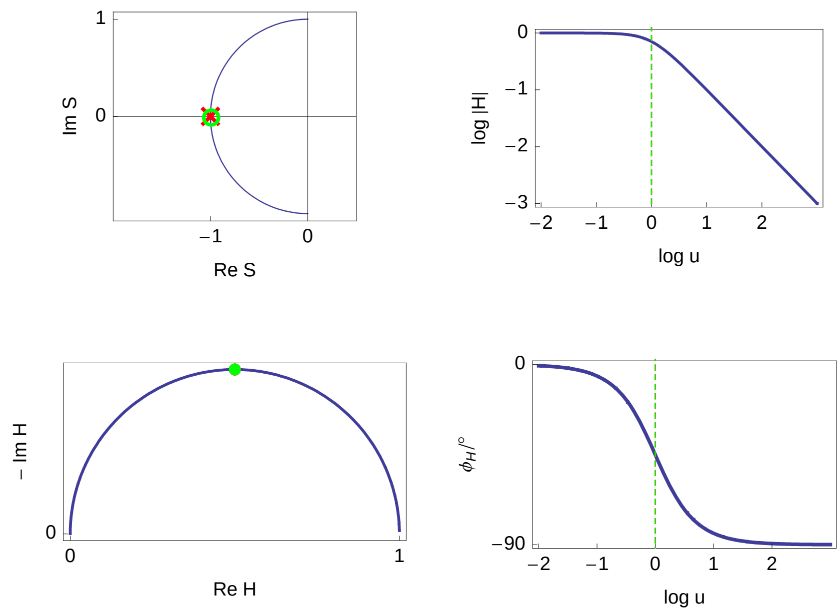

Figure 3.9: Pole-zero map, Nyquist, Bode (modulus and phase) of the reduced generalized second-order transfer function with multiple poles $H^*(u) = (1 + T\,\mathrm{i}\,u)/(1 + 2\,\zeta\,\mathrm{i}\,u + (\mathrm{i}\,u)^2)$. $\zeta = 1$, $T = 1$.

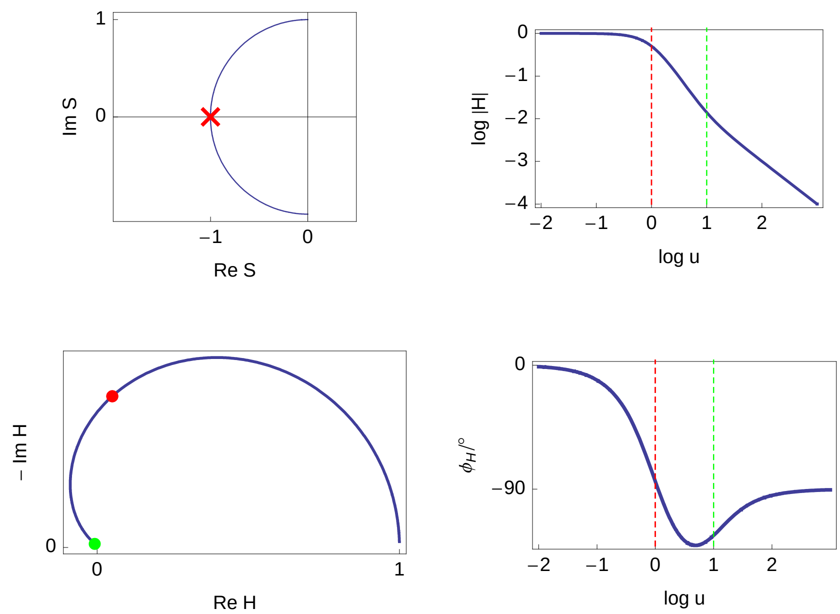

Figure 3.10: Pole-zero map, Nyquist, Bode (modulus and phase) of the reduced generalized second-order transfer function with multiple poles $H^*(u) = (1 + T\,\mathrm{i}\,u)/(1 + 2\,\zeta\,\mathrm{i}\,u + (\mathrm{i}\,u)^2)$. $\zeta = 1$, $T = 1$. Zero not shown in the pole-zero map

3.2.7 Real poles $\zeta > 1$

- 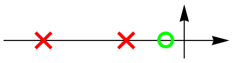 : Fig. 3.11,
- 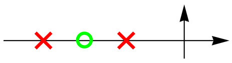 : Fig. 3.12,
- 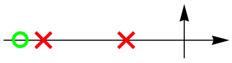 : Fig. 3.13.

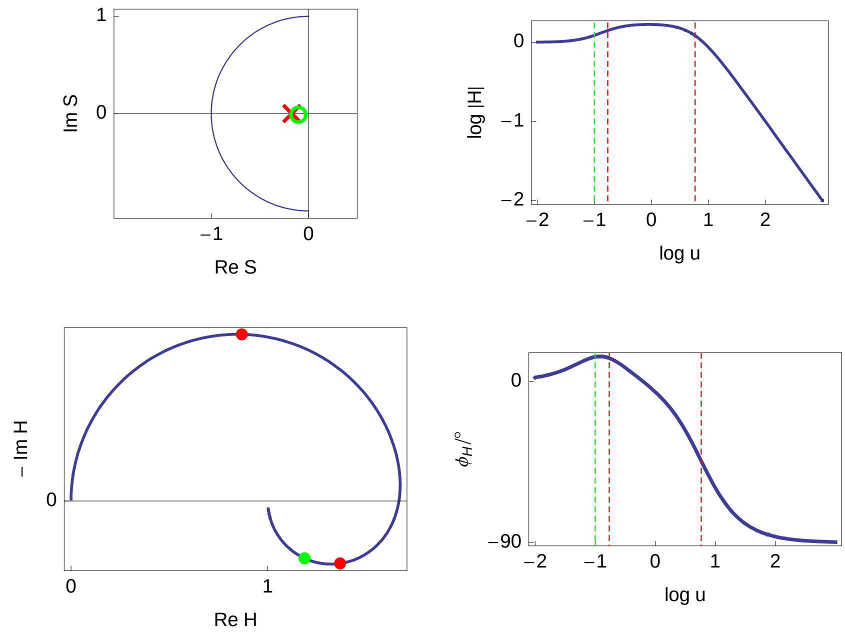

Figure 3.11: Pole-zero map, Nyquist, Bode (modulus and phase) of the reduced generalized second-order transfer function with real poles $H^*(u) = (1 + T\,\mathrm{i}\,u)/(1 + 2\,\zeta\,\mathrm{i}\,u + (\mathrm{i}\,u)^2)$. $\zeta = 3$, $T = 10$.

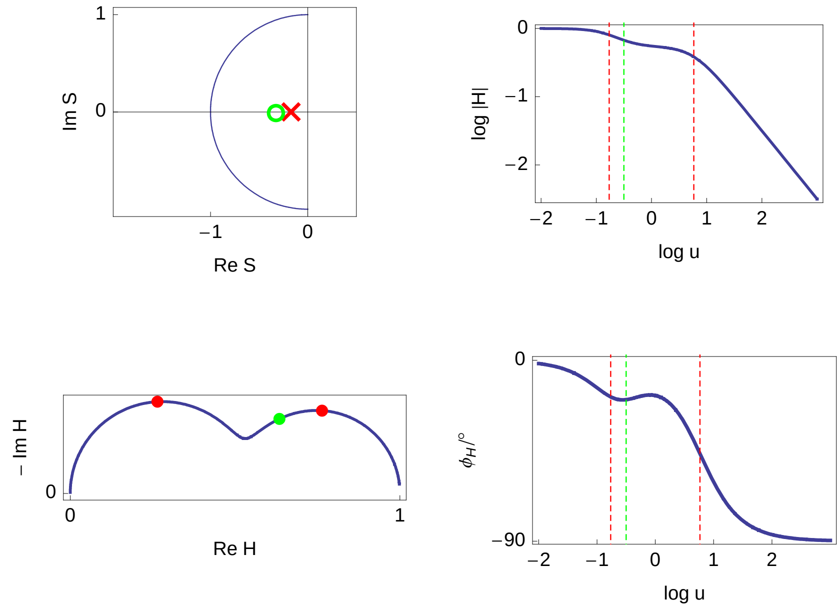

Figure 3.12: Pole-zero map, Nyquist, Bode (modulus and phase) of the reduced generalized second-order transfer function with real poles $H^*(u) = (1 + T\,\mathrm{i}\,u)/(1 + 2\,\zeta\,\mathrm{i}\,u + (\mathrm{i}\,u)^2)$. $\zeta = 3$, $T = 3.16$. One pole not shown in the pole-zero map.

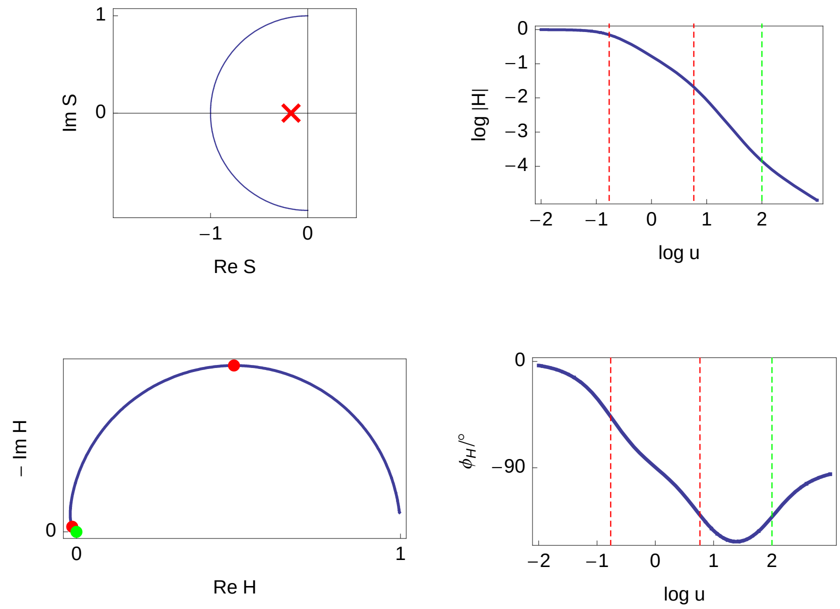

Figure 3.13: Pole-zero map, Nyquist, Bode (modulus and phase) of the reduced generalized second-order transfer function with real poles $H^*(u) = (1 + T\,\mathrm{i}\,u)/(1 + 2\,\zeta\,\mathrm{i}\,u + (\mathrm{i}\,u)^2)$. $\zeta = 3$, $T = 10^{-2}$. Zero and one pole not shown in the pole-zero map.

Chapter 4

Appendix: 3D-plot of transfer functions

4.1 3D-plot of modulus [4]

4.1.1 First order transfer function

$$H^*(S) = \frac{1}{1+S},\ S = \Sigma + \mathrm{i}\,u$$

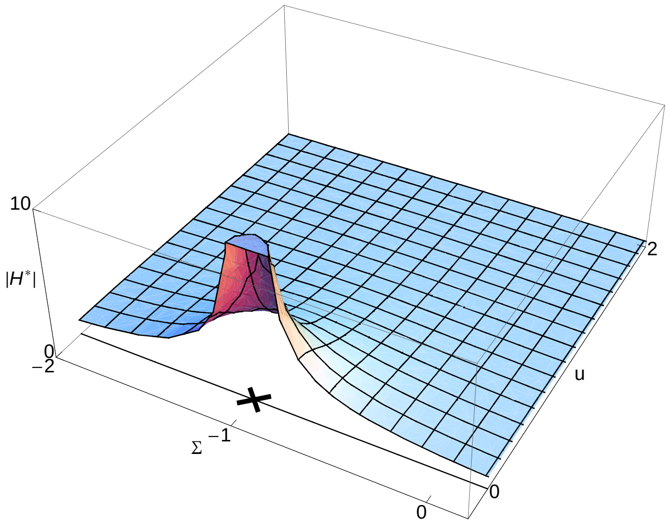

Figure 4.1: 3D-plot of the modulus of first order transfer function.

4.1.2 Second order transfer function

Complex poles

$$H^*(S) = \frac{1}{1+2\,\zeta\,S+S^2},\ S = \Sigma + \mathrm{i}\,u,\ \zeta < 1$$

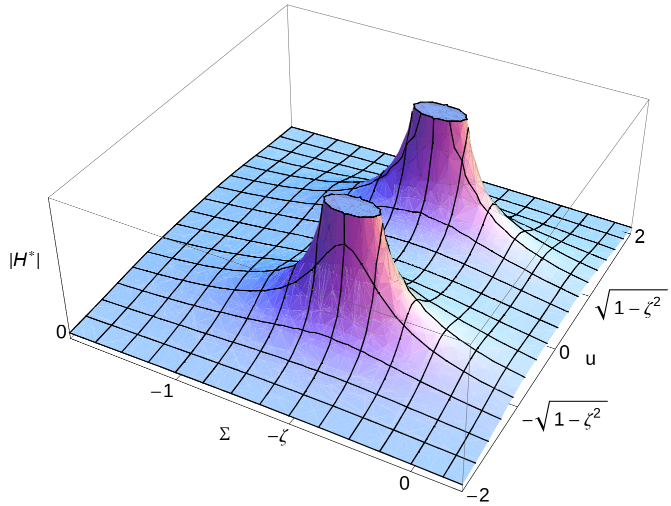

Figure 4.2: 3D-plot of the modulus of second order transfer function. Complex poles, $\zeta = 0.5$

Real poles

$$H^*(S) = \frac{1}{(1+S)\,(1+r_\tau\,S)},\; S = \Sigma + \mathrm{i}\,u$$

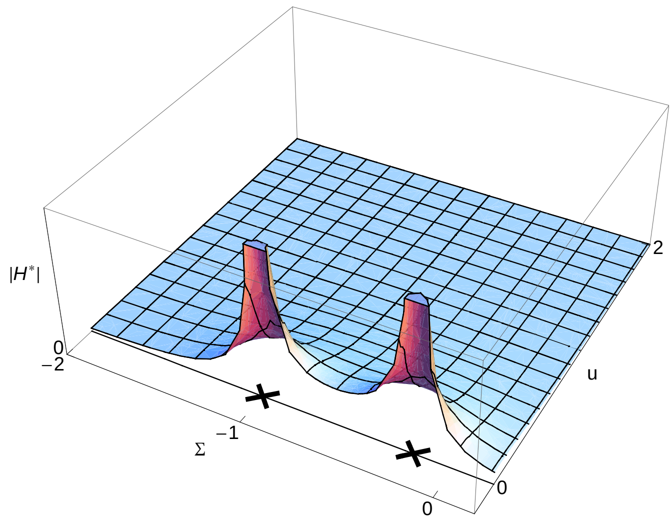

Figure 4.3: 3D-plot of the modulus of second order transfer function. Real poles, $r_\tau = 5$

Bibliography

[1] Control systems/system metrics. `http://en.wikibooks.org/wiki/Control Systems`.

[2] Cattarin, S., Comisso, N., Musiani, M., and Tribollet, B. The impedance of an electrode coated by a resistive film with a graded thickness. *J. Electrochem. Soc. 11* (2008), C27–C30.

[3] de Larminat, P., and Tomas, Y. *Automatique des systèmes linéaire. I. Signaux et systèmes*. Flammarion, Paris, 1975.

[4] Diard, J.-P., B. Le Gorrec, and Montella, C. Il n'y a pas que $j\,\omega$. In *Proceeding of the 7th Forum sur les Impédances Électrochimiques* (Montrouge, 1993), C. Gabrielli, Ed., pp. 133–138. `http://www.Electrochimie.org`.

[5] Diard, J.-P., B. Le Gorrec, Montella, C., and Montero-Ocampo, C. Second order electrochemical impedances and electrical resonance phenomenon. *Electrochim. Acta 37* (1992), 177–179.

[6] Diard, J.-P., B. Le Gorrec, Montella, C., and Montero-Ocampo, C. Calculation, simulation and interpretation of electrochemical impedance diagrams. part IV. Second-order electrochemical impedances. *J. Electroanal. Chem. 352* (1993), 1–15.

[7] Fournier, J., Wrona, P. K., Lasia, A., Lacasse, R., Lalancette, J.-M., Menard, H., and Brossard, L. *J. Electrochem. Soc. 139* (1992), 2372.

[8] Gille, J.-C., Decaulne, P., and Pélegrin, M. *Dynamique de la commande linéaire*. Dunod, Paris, 1991.

[9] Huang, V. M.-W., Vivier, V., Orazem, M. E., Pébère, N., and Tribollet, B. The apparent constant-phase-element behavior of a ideally polarized blocking electrode. *J. Electrochem. Soc 154* (2007), C81 – C88.

[10] Montero-Ocampo, C. *Impédances électrochimiques du second ordre. Exemple du mécanisme de Volmer-Heyrovský avec désorption chimique*. PhD thesis, Institut National Polytechnique de Grenoble, Grenoble, 1988.

[11] Orazem, M. E., Pébère, N., and Tribollet, B. *J. Electrochem. Soc 153* (2006), B129.

[12] Rodiguez-Presa, M. J., Tucceri, R. I., Florit, M. I., and Posadas, D. Constant phase element behavior int the poly(*o*-toluidine) impedance response. *J. Electroanal. Chem. 502* (2001), 82–90.

[13] Schuhmann, D. Étude phénoménologique à l'aide de schémas réactionnels des impédances faradiques contenant des résistances négatives et des inductances. *J. Electroanal. Chem. 17* (1968), 45–59.